ACTA METALLURGICA SLOVACA
2022, VOL. 28, NO. 4, 181-187

RESEARCH PAPER

EFFECTS OF ALUMINIUM ADDITION AND AUSTEMPERING TEMPERATURES ON AL-ALLOYED DUCTILE IRON MICROSTRUCTURE AND MECHANICAL PROPERTIES

Abdullahi Olawale Adebayo[1], Olawale Olarewaju Ajibola[1,3], Oluwasegun Eso Falodun[2,3], Sunday Gbenga Borisade[1], Adebayo Felix Owa[1], Oluwole Daniel Adigun[1], Akinlabi Oyetunji[4], Kenneth Kenayo Alaneme[3,4]*

[1]Department of Materials and Metallurgical Engineering, Federal University Oye-Ekiti, 371101 Oye-Ekiti, Nigeria.
[2]Department of Mechanical Engineering, Covenant University, 112233, Ota, Nigeria.
[3]Centre for Nanomechanics and Tribocorrosion, University of Johannesburg, 2094, Doornfontein, South Africa.
[4]Department of Metallurgical and Materials Engineering, Federal University of TechnologyAkure, 340001 Akure, Nigeria.

*Corresponding Author: abdullahi.adebayo@fuoye.edu.ng, +2348064837675, Faculty of Engineering. Federal University Oye-Ekiti, 371101 Oye-Ekiti, Ekiti State.

Received: 08.09.2022
Accepted: 27.11.2022

ABSTRACT

The research investigates the effect of varying amounts of aluminium (1.05, 1.575, 2.29, 3.02 and 3.74 wt.%) addition and heat treatment (austempering at 300, 350, 400 °C) on the microstructure and mechanical properties of ductile cast iron alloys. The graphitizing effects of the Al alloy and varied austempering temperatures on the hardness, tensile strength, and impact toughness of the ductile cast iron (DCI) were evaluated. The results of the influences of Al addition and heat treatment on the properties of the DCI determined were graphically presented while the characterization was done using ~~a~~ scanning electron microscope (SEM). The microstructures revealed that the addition of Al into the matrix brings about the precipitation of ferrite around the graphite nodules. The combined effects of the increase in Al content and austempering temperatures produced greater hardness values on the Al-alloyed DCI samples than the as-cast sample. The hardness values for the entire samples ranged from 27.25 to 57.03 BHN. Tensile strength increased with ~~an~~ increase in Al content and lower austempering temperatures, whereas, the impact toughness increased with increase in Al content and higher austempering temperature. The results of the research revealed that the addition of Al to ductile iron and austempering treatment led to an improvement in the hardness, tensile strength, and impact toughness of the alloys.

Keywords: Ductile cast iron; heat treatment; austempering; microstructure; mechanical properties

INTRODUCTION

Ductile cast iron (DCI) is a special class of cast iron that possesses appreciable level of ductility due to the presence of graphite nodules embedded in the ferrite/pearlite matrices. The material's properties can be improved by altering some processing parameters via heat treatment procedures [1–3]. In casting ductile iron, some of the parameters that influence solidification include melt-composition, Mg-treatment, and inoculation [4–7]. The cooling rate affects graphite structure formation and properties of the casting product [7]. The rare earth metals and elements such as Ce, Ca, Ni, Si, and Al promote graphite nucleation and growth, whereas, As, Bi, B, Sb, Sn, and Pb reduce the formation [4]. Pedro *et al.* [6] used FeSi and FeSiMg for inoculation and nodulation in a ladle with a nodulation pocket. Upadhyaya et al. [5] used Ce-Ca-Al-S-O-FeSi, Zr-Mn-Ca-Al-Ba-FeSi, and Sr-Al-Ca-FeSi as inoculants which were found to be very effective.

Ductile cast irons are very versatile materials for the automobile and automotive industries. The higher demand for DCIs than ordinary cast iron is principled on their suitability for different engineering applications including automobiles, automotive engines, cutting tools, rolls, dies, and gears. They are employed as structural materials in civil construction, agricultural and mining equipment [8–10] for their higher degree of ductility, high strength, toughness, as well as shock, corrosion and wear resistance; excellent castability, moderate damping capacity and good combination of strength, ductility and toughness [7]. The need for the reduction in the weight of automobile engines as requisite for fuel-saving has ignited research into the development of various types of new light materials. Whereas, the common types of light metals and alloys widely used for such purposes include Al, Mg, Ti [11], the addition of Al to cast iron would not only reduces the density but also plays the lead role in enhancing the mechanical properties such as the ductility, toughness, and formability [2].

Diverse works on various properties of austempered ductile cast iron (ADCI) and Aluminium-alloyed austempered ductile cast iron (AADCI) have been widely circulated. These include contact and bending fatigue behaviour; microstructure and abrasion wear behavior, wear and friction behaviors [12]. Pereira *et al.* [13]studied the mechanical properties such as ultimate tensile strength (UTS), yield strength (YS), elongation); Brinell hardness (HB) and microstructures of austempered ductile cast iron (ADCI) alloyed with Cu-Ni-Mn-Mo in hot air austempering cycles in a two-step mechanism. It was stated that alloying with small additions of Cu, Ni, Mn, and Mo

is more effective than significant addition of only one of these elements due to Cu and Ni having negative segregation, and Mn and Mo have positive segregation [14). The corrosion behaviors of steel, CI, DCI and ADCI of different alloying formations have been studied, and reported by authors [10, 15, 16].

Different heat treatment processes have contributed to the enhancement of diverse properties of DCI. The grains refinement and phase transformations have been achieved in many ways. ADCIs demonstrate more fascinating combinations of characteristics like low cost, elevated strength, fatigue and wear resistance compared with steels of the same hardness [17]. The hardness, strength and toughness are tripartite mechanical properties of repute that are much required in automobile engines, although, there are correlations and differences among these three properties [3, 18]. Austempering modifies the structure to getting more ductility with improved softness. Pereira *et al.*[13] and Putatunda [19] among others adopted the two-step austempering process on ADCI.

Despite the spectrum of literature reports that are available on diverse research undertaken so far on the DCI; it is unpleasant that research reports [20, 21] are very scarce on Al-DCI alloys and, austempered Al-DCI alloys. The combination of Al alloying and austempering on DCI is the major interest in the present work, due to various advantages acclaim to Al in the formation of AADCI. Al addition produces Al_2O_3 in the melt and forms a film layer on the outside surface of the casting, thus, provides the resistance against oxidation at elevated temperatures. The graphitizing potential of Al is next to silicon with a higher tendency to produce thin-wall castings of cast iron without eutectic carbide formation; thus, reducing the overall weight of the castings (cylinder block or cylinder head); owing to the density of aluminium and thinning the wall of the castings. Al addition provides aluminium complexes (more eutectic cells, higher strength) during solidification [21].

The work evaluates the production of aluminium base DCI alloy. It investigates the casting procedure, heat treatment processing parameter variations, the consequences of the processing parameter on the mechanical properties (toughness, strength, and hardness) of the derived Al-alloyed DCI, assessment of microstructures, phase transformations and interactions between the cast iron matrix and aluminium alloy.

2. MATERIAL AND METHODS

2.1 Materials Fabrication and Preparation

The Al-DCI samples were produced in the foundry laboratory at the EMDI, Akure, Nigeria with high purity raw materials using the rotary furnace. The liquid cast iron was tapped into a preheated ladle containing Al chips and Fe-Si-Mg alloy at tapping temperature of 1500 °C for the Al alloying and nodulizing process; before the inoculation with FeSi addition in the same ladle as the mixture is agitated mechanically at 1400 °C before being finally poured into the sand moulds. Rectangular shape ingots were cast, solidified, cooled to room temperature in the mould as described by [22, 23]. X-Ray Fluorescence (XRF) analyzer (Rigaku ZSX Primus II model) was used to determine the chemical composition of cast DCI samples as shown in **Tab. 1**.

2.2 Heat Treatment Procedures

In this study, the samples were charged into the salt bath (50% $KNO_3$and 50% $NaNO_3$) and slowly heated to austenitizing temperature (γ_{Temp}) of 850°C from 25°C room temperature, held at the γ_{Temp} for homogenization and austempered. The procedure for the austempering process is as shown in **Fig. 1** which includes: i. steady heating of the samples in a molten salt bath (at the rate of 11°C/min to γ_{temps} of 850 °C for 75 mins); ii. held at 850 °C austenitizing temperature for homogenization for 15 mins; iii. removal from the furnace and quickly quenched in another molten salt bath to avoid pearlite transformation within 1 - 3 secs; iv. holding at the austempering temperature in the molten salt bath for complete isothermal transformation to ausferrite at 300, 350, and 400 °C for 90 mins; v. finally removed and cooled in still air.

2.3 Microstructure and Hardness Test

The heat treated samples for hardness test were sliced to10mm (breadth) x 10mm (thickness) x 12mm (length) using the automatic cutting machine (Brillant 220, ATM, Germany). The sample surfaces were prepared for hardness and microstructure analysis. Grinding was done using Aka-Allegan 9 plate after smoothing with SiC grit paper (P320) and fine poly suspension (Dia-max 9 μm). To obtain a very smooth and mirror-like finishing surface, the polishing entails using an Aka-Moran plate with 3 μm poly suspension and later, Aka-Chemal plate with 0.2 μm fumed silica respectively on the automatic polishing machine (Saphir 550, ATM, Germany).

The microstructural and phase analysis of the produced Al-DCI was characterized using TESCAN VEGA3 scanning electron microscopy equipped with energy dispersive spectroscopy (EDS) and PANalytical Empyrean diffractometer (PW1710), with monochromatic Cu target Kα radiation at 40 kV and 40 mA. The constituent phases of the Al-DCI were revealed using Highscore X'Pert Software. The hardness test was done for the produced Al-DCI samples by using the Atico India Brinell hardness testing machine. Each of the specimens was first cleaned from dust, dirt and grease, then, placed and securely mounted on the machine. The ball indenter was impressed with an applied load of 10N for a dwell period of 15 secs. The Brinell hardness scale was read after the pointer had come to rest. The indentation was viewed through a microscope and the diameter was measured with the attached micrometer. The procedure was repeated three times and average results were taken.

2.4 Tensile Strength Test Procedures

Three tensile test samples of gauge length of 28 mm with gauge diameter of 7 mm were machined from the same class each of DCI and Al-DCI alloys (M1, M2, M3, M4, M5, M6), and the tests were carried out following ISO 6892-1 (2016). The average values of results were obtained as the tensile strength of the alloys. A table-top universal tensiometer of Model KPL 2000-1 with a self-aligned Instron 8800 digital controlled panel was used to perform the tensile test. Test specimens were clamped on opposite ends on the Instron machine cramp and stretched at a slow constant rate until fracture.

2.5 Impact Toughness Test

The impact strength was determined with the aid of Tinius Olsen model JBN-300 capacity impact testing machine with a direct reading gauge. Three specimens each of size (10x10x50) mm with v-notch at the centre at an angle of 45° and a striking load of 75 kg weight was also used for each sample, and the average values determined in accordance with ISO 148-1 (2016) and JISG0202-1987specifications. To calculate energy E absorbed on the Charpy impact test, equation 1 was used.

$$E(J) = WgR(\cos\beta - \cos\alpha) - L \quad (1.)$$

Where: **W** = mass of hammer (kg), **g** = acceleration due to gravity (m/s^2), **R** = length of arm (m), **L** = energy loss to impact (J), **α** = angle of fall (°) and **β** = angle of the swing (°)

3. RESULTS AND DISCUSSION

3.1 Characterization of Samples

The effects of chemical composition on the ductile cast iron are similar to that of grey iron with quantitative and qualitative differences in the influence on graphite morphology. The presence of minor elements like Cr, Cu, Mg, Mn and Ca appreciably modified the microstructure of graphite morphology and matrix structure in that; they ~~can~~ encouraged the spheroidization of graphite [4, 7, 14, 19] or negatively influence flake graphite shape [22] which is the single most vital feature responsible for the enhancement of the mechanical properties of cast iron as obtained in the study and illustrated in the microstructures. Fig. 1 shows the procedures for the single step austempering processes adopted in the study. M1~~is~~was as-cast DCI without Al addition, though, contains Al as a trace element (0.024%). M2 to M6 have an increasing amount of Al **(**1.05, 1.575, 2.29, 3.02 and 3.74 wt.%) in the alloyed ductile cast iron produced [23] and were compared with the as-cast sample.

Tab. 1 Chemical composition of cast Al-DCI samples

Alloy	Chemical Composition (wt.%)										
	Cr	Cu	Si	Mg	Mn	Ca	Al	C	Fe	P	S
M1	0.102	0.121	2.920	0.107	0.400	0.003	0.024	3.795	Bal.	0.073	0.076
M2	0.127	0.143	2.460	0.053	0.376	0.025	1.050	3.642	Bal.	0.066	0.041
M3	0.106	0.139	2.290	0.075	0.320	0.001	1.575	3.549	Bal.	0.052	0.026
M4	0.109	0.135	2.210	0.078	0.377	0.002	2.290	3.527	Bal.	0.062	0.019
M5	0.102	0.138	2.090	0.010	0.372	0.001	3.020	3.411	Bal.	0.074	0.013
M6	0.103	0.134	2.010	0.009	0.381	0.001	3.740	3.408	Bal.	0.068	0.010

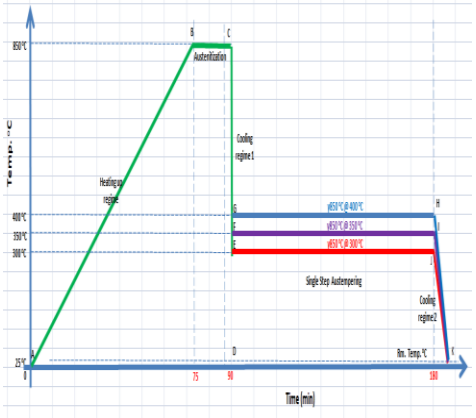

Fig. 1 Procedure for the heat treatment of the samples

3.2 Microstructural and Phase Evaluation

The combined effects of Al addition and the austempering on the trends of microstructural transformations at different temperatures are presented in Figs. 2-5. The microstructures displayed even distribution of graphite nodules within the DCI matrices. This may be the right quality required in DCI material to have high impact strength, giving room for the applied stresses to be distributed evenly throughout the bulk component in addition to high material yield strength. According to Hernandez-Rivera et al. [25], as the treatment proceeds for 15 mins, the carbon content in the austenite increases to allow the formation of a more significant portion of stabilized austenite in the final microstructure. Graphite nodules appeared as dark round areas on the un-etched micrographs [6].

Microstructures in Fig. 2 affirms that post inoculation is a result-oriented method for DCI production; which its efficiency depends on the early nucleating potential of the melt. The as-cast sample was not austempered, thus, Fig. 2a-f portrays the characteristic effects of increasing the addition of Al content on DCI microstructures. This also shows the trends of dependence on the formation of pearlites as the Al content increased. Fig. 2a illustrates the even distribution of graphitic nodules within the iron matrix. The observation of pearlites emanated with the addition of 1.05 wt.% Al to as-cast without Al addition. Thereafter, a significant appearance of pearlites was seen in the microstructures as shown in Fig. 2d-f.

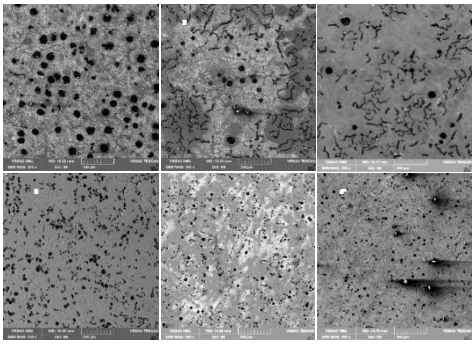

Fig. 2 SEM micrographs of M1-M6 of cast with various Al content; (a) As-Cast without Al (b) 1.05 wt.% Al (c) 1.575 wt.% Al (d) 2.29 wt.% Al (e) 3.02 wt.% Al and (f) 3.74 wt.% Al

Fig. 3a-f shows the trends of reliance and the diversities in the formation of Al-alloyed DCI microstructures as the Al content increased at 300ºCaustempering temperature. The result revealed that besides the graphitic nodules within the DCI matrix; graphites are noticed to be precipitated along the grain boundaries in many considerable quantities in the Al-alloyed DCI alloys in Fig. 3b-f. The number of nodules is relatively small when 1.05 wt.% Al is added to as-cast DCI. This established the fact that Al presence substantially alters the graphite morphology and matrix structure through spheroidization as shown in Fig. 3d-e.

At 350 °C austempering, the microstructure of the cast sample in Fig. 4a does not show a significant difference as with 300 °C. In Fig. 4a, some ferrite was observed in the bulk matrix of DCI. However, the addition of 1.05 – 3.74 wt.% Al revealed the precipitation of ferrite around the graphite nodules rather

than in the bulk matrix of the cast samples. The matrix is mainly pearlite and ferrite resembling concentric shells around graphite nodules [5, 23].These properties are due to the characteristic of ADI microstructure, which consists of graphite nodules dispersed in a matrix of acicular ferrite and retained austenite ("ausferrite") [17, 23].

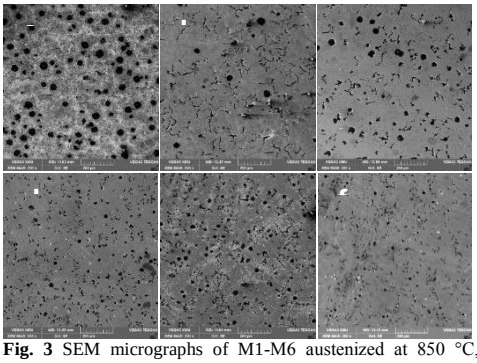

Fig. 3 SEM micrographs of M1-M6 austenized at 850 °C, austempered at 300 ºC for 90 mins.; (a) Cast without Al (b) 1.05 wt.% Al (c) 1.575 wt.% Al (d) 2.29 wt.% Al (e) 3.02 wt.% Al and (f) 3.74 wt.% Al

Fig. 5a-f presents the morphology at 400 °C austempering of the cast samples. However, it was observed that there was precipitation of ferrite around the graphite nodules in the matrix of the cast samples. The changes are evidence of microstructural transformations during the austempering processes, thus, establishing the wide temperature difference role in quenching and the austempering process.

The micrographs generally revealed the presence of nodularity of graphite and the morphology of pearlite. The ferrite regions around graphite nodules are due to the diffusion of carbon towards the graphitizing area [5]. Since a material's strength depends on its microstructure, the engineering processes can alter it. A variety of strengthening mechanisms such as work-hardening, solid solution strengthening, precipitation hardening, and grain boundary strengthening alter the strength of a material and can be quantitatively and qualitatively explained. In all instances, the microstructure after the heat treatment consisted of graphite nodules and carbides within an ausferritic matrix.

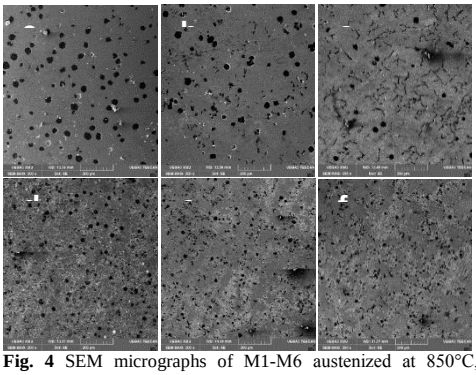

Fig. 4 SEM micrographs of M1-M6 austenized at 850°C, austempered at 350°C for 90 mins.; (a) Cast without Al (b) 1.05 wt.% Al (c) 1.575 wt.% Al (d) 2.29 wt.% Al (e) 3.02 wt.% Al and (f) 3.74 wt.% Al

The nodules and carbides remained unchanged reflecting the stability provided by the alloying elements. Moreover, all heat-treated microstructures showed graphite nodules and carbides immersed in an ausferritic matrix of the Al-alloyed austempered ductile cast irons (AADCI) with no variations observed on their characteristics [1, 6, 23].

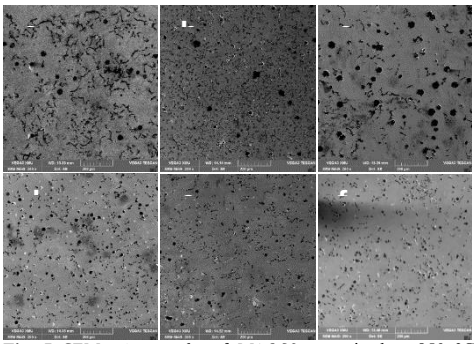

Fig. 5 SEM micrographs of M1-M6 austenized at 850 °C, austempered at 400°C for 90 mins.; (a) Cast without Al (b) 1.05 wt.% Al (c) 1.575 wt.% Al (d) 2.29 wt.% Al (e) 3.02 wt.% Al and (f) 3.74 wt.% Al

The earlier works of Adebayo et al. [12, 23] had reported the presence of theformation of some intermetallics compounds which showed the presence of Al-carbide phases in all the samples that contain Al as indicated in the form of intermetallic compounds of Al such as Al_4SiC_4, Al_4C_3 and $MgAl_2C_2$; in addition to Fe_3C and Fe_2C. This correlates and validates the carbide formation reported by Pimentel [26] on Niobium carbide and Chromium carbides (as eutectic of M_3C) that were formed from the addition of Nb and Cr to cast iron. Other intermetallic compounds earlier identified includeMg_2Si, $Al_2Fe_3Si_4$, Al_5FeSi, AlFe, $AlFe_3$, Al_2FeSi and Al_8FeSi.

3.3 Mechanical properties of the as-cast DCI and Al-alloyed DCI

Fig. 6 shows the hardness of M1-M6 austenitized at 850 °C and austempered at 300, 350 and 400 °C for 90 mins; the hardness increases with an increase in Al content and with a decrease in austempering temperature. In each instance, the combined effects of increased Al content and austempering temperatures produced greater hardness values on the Al-alloyed DCI samples than the as-cast sample. The hardness

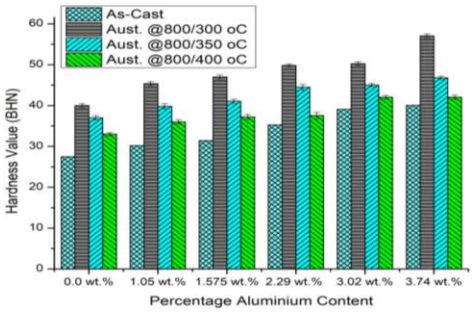

Fig. 6 Hardness of M1-M6 austenitized at 850 ºC and austempered at 300, 350 and 400 ºC for 90 mins.

imparted ranged between 27.25 ~ 40.05 BHN for the as-cast sample, much lower than the hardness obtained from the heat treatment processes (40~57.03 BHN) at 300 °C; (37~46.8 BHN) at 350°C and (33.5~42.05 BHN) at 400°C respectively. The Al addition yielded similar results to having improved hardness and impact toughness of ADI as it did with 0.2 wt.% Nb addition [27]. The austempered samples may also experience a high increase in hardness because of the formation of strain-induced [17].

The tensile test conducted was to establish the influence of the Al additions on the enhancement of the tensile strength of DCI. The test is a universal method to evaluate the mechanical properties of a material and give some clear information on the microstructure and chemistry (composition, phases) [28]. In this study, a tensile test was selected to analyze the qualities of cast iron products required in making automobile engine parts, relative to their tensile strength and greatly dependent on the carbon content. **Fig. 7** presents the result of tensile strength of varying Al-alloy DCI samples austenitized at 850 °C and austempered at 300, 350 and 400 °C for 90 mins. The tensile strength obtained ranged between 324.883 ~ 402.13 Nmm^{-2} for the as-cast sample; which is lower than the minimum values of tensile strength obtained from the austempering treatment processes (720 ~790 Nmm^{-2}) at 300 °C; (710 ~770 Nmm^{-2}) at 350 °C and (710.5 ~745.14 Nmm^{-2}) at 400 °C; implying the strengthening effect of silicon in line with reported literature [29, 30]. Thus, M3-M6 can stand the minimum tensile strength requirement for agricultural machinery, automotive engine, mining, railway and other fields due to its high tensile strength (≤1600 MPa) and good impact toughness (≥ 100 J/cm^3) [31, 32]. For all cases of increased Al content and austempering temperatures; the tensile strength obtained for the M1-M6 were almost or more than double the values (695.78 ~ 790 Nmm^{-2}) as compared with the as-cast specimen (324.88 ~ 402.13 Nmm^{-2}). However, the tensile strength increased with an increase in Al content. This is due to the precipitates of fine ferrite and pearlite with embedded graphite in the as-cast structure observed in different proportions. The more the precipitates, the more the strength increases. For the austempered samples, aside the influence of Al, the higher degree of under-cooling favour nucleation and growth of finer ferrite and austenite (finer ausferrite) resulting in higher yield and tensile strengths but at the expense of ductility.

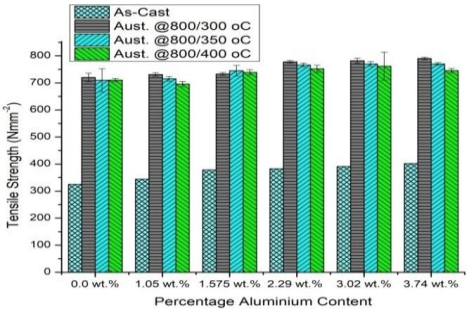

Fig. 7 Tensile Strength of M1-M6 austenitized at 850 ºC and austempered at 300, 350 and 400 ºC for 90 mins.

The impact toughness of the M1- M6 specimen was austenitized at 850 °C and austempered at 300, 350 and 400 °C for 90 mins are shown in Fig. 8. The as-cast samples have lower toughness as compared with the Al-DCI resulting from the effects of both increased Al content and austempering temperatures. The impact toughness decreased with increase in Al content and with a decrease in austempering temperature for both control samples and heat-treated samples. It is fundamental that; pearlite increases strength, hardness but reduces impact energy. An increase in the ferrite portion (alpha iron) increases impact toughness because ferrite (alpha iron) has good ductility (plasticity) and an excellent ability to resist the impact energy at low temperatures. An increase in nodules size and nodules count (Figs. 2-5) decreases the impact toughness properties. The impact energy is between 42.5 ~ 55.5 Jm^{-3} for the as-cast sample, being lower than the ranges of impact energy obtained from the austempering processes (50 ~ 60 Jm^{-3}) at 300 °C; (56 ~ 61.4 Jm^{-3}) at 350 °C and (57.5 ~ 64 Jm^{-3}) at 400 °C.

In the present result, the microstructure obviously influences mechanical properties and fracture behaviour. The degree of under-cooling has a pronounced effect on the volume of carbon diffusion. The austempering at a lower degree of under-cooling would enhance carbon diffusion. Thus, an increase in austempering temperature assists the carbon diffusion process to stabilize the non-transforming austenite; hence, the higher carbon content in the austenite (γcCc parameter). An increase in this parameter further improves the fracture toughness of the materials [9]. The presence of pearlite increases strength, hardness but reduces impact energy. Engineering design stresses obtained from the ultimate strength or yield point values of the materials give safe and reliable results only for the case of static loading. As illustrated in Figs. 6 to 8, error bars for each plot provide the upper and lower limit (maximum and minimum amount) of hardness (Fig. 6), tensile strength (Fig. 7) and impact toughness (**Fig. 8**) obtained from each of wt.% Al values.

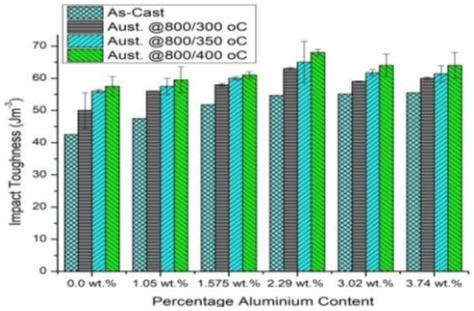

Fig. 8 Impact Strength of M1- M6 austenitized at 850 ºC and austempered at 300, 350 and 400 ºC for 90 mins.

CONCLUSIONS

The conclusions that can be established in accordance with the obtained results are as follows:

i. The microstructures revealed that the addition of Al into the matrix brings about the precipitation of ferrite around the graphite nodules.
ii. The addition of Al to ductile cast iron increases the hardness and tensile strength of the alloys.
iii. Austempering further improves the tensile and hardness properties of the alloy which increase with a higher degree of under-cooling.
iv. Austempering also improves the impact toughness of the alloy but decrease with increase in the degree of under-cooling.

Acknowledgement: The authors express their sincere gratitude to the Centre of Nanomechanics and Tribocorrosion, University of Johannesburg, South Africa for providing the laboratory facilities for this research.

REFERENCES

1. A. O. Adebayo: Processing and Characterization of Austempered Aluminium-Alloyed Ductile Irons for Automobile Applications, The Federal University Of Technology Akure, Nigeria, 2019.
2. S. Samaddar, T. Das, A. K. Chowdhury, M. Singh: Manufacturing of Engineering Components with Austempered Ductile Iron–A Review, Materials Today: Proceedings, 5(11), 2018, 25615–25624. https://doi.org/10.1016/j.matpr.2018.11.001.
3. Y. Yürektürk, M. Baydoğan: Characterization of Ferritic Ductile Iron Subjected to Successive Aluminizing and Austempering, Surface and Coatings Technology, 347, 2018, 142–149. https://doi.org/10.1016/j.surfcoat.2018.04.083.
4. R. Källbom, K. Hamberg, M. Wessén, L-E, Björkegren: On the Solidification Sequence of Ductile Iron Castings Containing Chunky Graphite, Materials Science and Engineering: A, 413-414, 2005, 346–351. https://doi.org/10.1016/j.msea.2005.08.210.
5. R. Upadhyaya, K. K. Singh: Effect of Some Inoculants on the Structure and Properties of Thin Wall Ductile Iron, Materials Today: Proceedings, 5(2), 2018, 3595–3601. https://doi.org/10.1016/j.matpr.2017.11.609.
6. D. I. Pedro, A. D. Mandri, R. C. Dommarco: Optimization of the Rolling Contact Fatigue (RCF) Performance of Carbidic Austempered Ductile Iron (CADI), Tribology International, 2020, 143. https://doi.org/10.1016/j.triboint.2019.106076.
7. P. B. Chikali and V. D. Shinde, Analysis of Machinability in Ductile Iron Casting, Materials Today: Proceedings, 2020, 27, 584-588. https://doi.org/10.1016/j.matpr.2019.12.064.
8. F. Concli: Austempered Ductile Iron (ADI) for Gears: Contact and Bending Fatigue Behavior, Procedia Structural Integrity, 2018, 8, 14–23. https://doi.org/10.1016/j.prostr.2017.12.003.
9. J. Yang, S. K. Putatunda: Effect of Microstructure on Abrasion Wear Behavior of Austempered Ductile Cast Iron (ADI) Processed by a Novel Two-Step Austempering Process, Materials Science and Engineering: A, 2005, 406(1–2), 217–228. https://doi.org/10.1016/j.msea.2005.06.036.
10. C.-H. Hsu, M.-L. Chen: Corrosion Behavior of Nickel Alloyed and Austempered Ductile Irons in 3.5% Sodium Chloride, Corrosion Science, 2010, 52(9), 2945–2949. https://doi.org/10.1016/j.corsci.2010.05.006.
11. H. Yuncheng, W. You, P. Zhaoyi, Y. U. Lili: Influence of Rare Earth Nanoparticles and Inoculants on Performance and Microstructure of High Chromium Cast Iron, Journal of rare earths, 2012, 30(3), 283–288. https://doi.org/10.1016/S1002-0721(12)60038-6.
12. A. O. Adebayo, A. Oyetunji, K. K. Alaneme: Microstructural Characteristics, Mechanical and Wear Behaviour of Aluminium-Alloyed Ductile Irons Subjected To Two Austempering Processes, Acta Polytechnica, 2020, 60(3), 185–196. https://doi.org/10.14311/AP.2020.60.0185.
13. L. Pereira, R. F. do Amaral, M. W. Júnior, V. K. de Barcellos: Microstructural and Mechanical Properties of Cu-Ni-Mn-Mo Austempered Ductile Iron Obtained from Two-Step Hot Air Austempering, Journal of Materials Research and Technology, 2020, 9(3), 3055-3063. https://doi.org/10.1016/j.jmrt.2020.01.036.
14. B. Y. Lin, E. T. Chen, T. S. Lei: The Effect of Segregation on the Austemper Transformation and Toughness of Ductile Irons, Journal of materials engineering and performance, 1998, 7(3), 407–419. https://doi.org/10.1361/105994998770347864.
15. H. Zhang, L. Zhao, D. Liu, J. Wang, X. Zhang, C. Chen: Early Period Corrosion and Scaling Characteristics of Ductile Iron Pipe for Ground Water Supply with Sodium Hypochlorite Disinfection, Water Research, 2020, 115742. https://doi.org/10.1016/j.watres.2020.115742.
16. X.-H. Sun, X.-B. Zuo, G.-J. Yin, K. Jiang, Y.-J. Tang: Electrochemical and Microscopic Investigation on Passive Behavior of Ductile Iron in Simulated Cement-Mortar Pore Solution, Construction and Building Materials, 2017, 150, 703–713. https://doi.org/10.1016/j.conbuildmat.2017.06.042.
17. K. H. S. Silva, J. R. Carneiro, R. S. Coelho, H. Pinto, P. Brito: Influence of Shot Peening on Residual Stresses and Tribological Behavior of Cast and Austempered Ductile Iron, Wear, Elsevier, 2019, 440, 203099. https://doi.org/10.1016/j.wear.2019.203099.
18. T. Ikeda, N. Noda, Y. Sano: Conditions for Notch Strength to Be Higher than Static Tensile Strength in High–Strength Ductile Cast Iron, Engineering Fracture Mechanics, 2019, 206, 75–88. https://doi.org/10.1016/j.engfracmech.2018.11.034.
19. S. K. Putatunda: Development of Austempered Ductile Cast Iron (ADI) with Simultaneous High Yield Strength and Fracture Toughness by a Novel Two-Step Austempering Process, Materials Science and Engineering: A, 2001, 315(1–2), 70–80. https://doi.org/10.1016/S0921-5093(01)01210-2.
20. S. M. A. Boutorabi, J. M. Young, V. Kondic: Austempering Kinetics of Spheroidal Graphite Aluminum Cast Iron [J], International Journal of Engineering, 1995, 6(2a), 45.
21. S. M. M. Kashani, S. M. A. Boutorabi: As-Cast Acicular Ductile Aluminum Cast Iron, Journal of Iron and Steel Research International, 2009, 16(6), 23–28. https://doi.org/10.1016/S1006-706X(10)60022-2.
22. O. J. Akinribide, S. O. Akinwamide, O. O. Ajibola, B. A. Obadele, S. O. Oluwagbenga Olusunle, and P. A. Olubambi, Corrosion Behavior of Ductile and Austempered Ductile Cast Iron in 0.01 M and 0.05 M NaCl Environments., Procedia Manufacturing, 2019, 30, 167–172. https://doi.org/10.1016/j.promfg.2019.02.024.
23. A. O. Adebayo, K. K. Alaneme, A. Oyetunji: Structural Characterization and Mechanical Properties of Rotary Melting Furnace Processed Aluminium Alloyed Ductile Irons, Journal of Taibah University for Science, 2019, 13(1), 248–257. https://doi.org/10.1080/16583655.2018.1560701.
24. O. O. Ajibola, D. T. Oloruntoba, B. O. Adewuyi: Metallurgical Study of Cast Aluminium Alloy Used in Hydraulic Brake Calliper, International Journal of Innovation and Scientific Research, 2014, 8(2), 324–333.
25. J. L. Hernández-Rivera, R. E. C. Cambranis, A. De la Garza: Study of Microstructural Evolution and Mechanical Properties Exhibited by Non Alloyed Ductile Iron during Conventional and Stepped Austempering Heat Treatment, Materials & Design, 32(10), 2011, 4756–4762. https://doi.org/10.1016/j.matdes.2011.06.030.
26. A. S. O. Pimentel, W. L. Guesser, W. J. R. C. da Silva, P. D. Portella, M. Woydt, J. Burbank: Abrasive Wear Behavior of Austempered Ductile Iron with Niobium Additions, Wear, 440-441, 2019, 203065. https://doi.org/10.1016/j.wear.2019.203065.
27. L. Chang, Y. Yan, X. Chen, Q. Hua, Q. Zhai: Effects of Niobium Alloying on the Microstructure and Mechanical Properties of Bainite Ductile Iron, *EPD Congress*, Wiley Online Library, 2014, 339–344.
28. A. C. Melado, A. S. Nishikawa, H. Goldenstein, M. A. Giles, P. A. S. Reed: Effect of Microstructure on Fatigue Behaviour of Advanced High Strength Ductile Cast Iron Produced by Quenching and Partitioning Process, International Journal of Fatigue, 104, 2017, 397–407. https://doi.org/10.1016/j.ijfatigue.2017.07.009.
29. T. Umetani, T. Ikeda, N. Sura, K. Ashizuka, T. Nemoto, H. Takada, K. Ogi, Tensile Strength, Fatigue Strength and Impact Strength of Solution Strengthened High Silicon Ferritic Ductile Cast Iron, Journal of Japan Foundry Engineering Society, 86(1), 2014, 36–42. https://doi.org/10.11279/jfes.86.36.

30. P. Weiß, A. Tekavčič, A. Bührig-Polaczek, Mechanistic Approach to New Design Concepts for High Silicon Ductile Iron, Materials Science and Engineering: A, 713, 2018, 67–74. https://doi.org/10.1016/j.msea.2017.12.012.
31. T. Yoshimoto, T. Matsuo, T. Ikeda: The Effect of Graphite Size on Hydrogen Absorption and Tensile Properties of Ferritic Ductile Cast Iron, Procedia Structural Integrity, 14, 2019, 18–25. https://doi.org/10.1016/j.prostr.2019.05.004.
32. A. O. Adebayo and A. Oyetunji, Production of Ductile Iron from Waste Sleeve Scraps for Automobile Applications, FUOYE Journal of Engineering and Technology, 2(1), 2017, 72-77. https://doi.org/10.46792/fuoyejet.v2i1.61.